J. Mol. Sci.
(Wuhan, China) Vol.1, No.2, (1983)

STABILIZING CYCLIC OZONE THROUGH TRANSITION METAL COMPLEXATION

Sung Shen-shu and Roald Hoffmann*
Department of Chemistry, Cornell University, Ithaca, New York 14853

Recived June 25, 1983

ABSTRACT

Equilateral triangular cyclic ozone, an unstable six π-electron system, can be stabilized by complexation with one or two d^6 ML_3 or C_{3v} ML_4 fragments, or on top of an $Fe_3(CO)_9$ unit. The binding of cyclic O_3 to these transition metal fragments is not as effective as that of P_3^{3-}, but may be sufficient for observation of such complexes.

SINCE the 1960's a number of *ab initio* calculations on ozone have been carried out. The results of these calculations show that there may be another minimum point on the potential energy curve for O-O-O bending besides the normal O_3 structure, with an O-O-O angle of 117°.[1] This minimum point is at the equilateral triangle geometry, 1a. This cyclic or ring state of O_3 is 28 to 35 kcal/mol above the normal bent ground-state of O_3, 1b, only a few kcal/mol above the energy required for dissociation of normal O_3 into O_2+O. The conversion of the cyclic and bent isomers is formally a forbidden reaction. However, when configuration interaction is included in the calculation the barrier to ring-opening, becomes small.

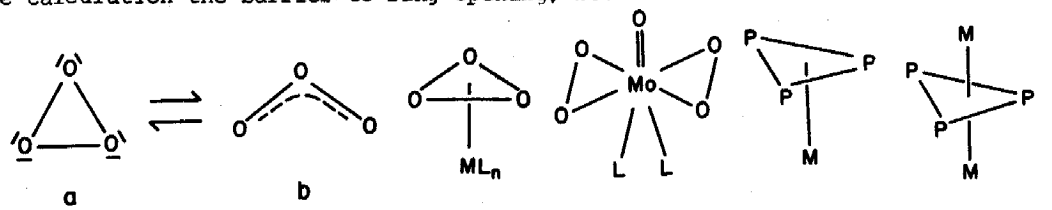

Cyclic ozone, or for that matter its SO_2 or S_3 analogue, is thus a so far nonexistent molecule, clearly of little thermodynamic or kinetic stability. This makes it a natural candidate for stabilization as a transition metal complex, 2. Numerous molecules or fragments of little stability have in fact been stabilized as transition metal complexes. Abundant cyclobutadiene, trimethylenemethane, acyl complexes, just to name a few examples, testify to this stratagem for stabilization.

The experimental evidence for ozone stabilization is nonexistent. One indirect piece of evidence one might have sought is oxo-peroxo scrambling in complexes in which both common oxygen ligands are found, e.g. the molybdenum (VI) com-

plex 3. In fact Sharpless and coworkers,[2a] in the course of a study of the mechanism of olefin epoxidation, prepared some 3 labeled with ^{18}O exclusively at the oxo atom. They found no oxo-peroxo label exchange under ambient conditions, thus excluding easy access to a cyclic ozone structure. Similar conclusions have been reached recently by Postel Riess et al.[2b]

Much more encouraging has been the synthesis in recent years of several cyclotriphosphorus, P_3, complexes;[3] 4 and 5 are examples. In this paper we explore theoretically the probability of stabilization of cyclic ozone by transition metal complexation.

The Electronic Structure of Cyclic Ozone

THE energy levels of cyclic ozone are shown in Fig.1. In our extended Hückel calculation (see Appendix for details) we assumed an O-O separation 1.50Å, based on an approximate figure from *ab initio* optimizations and the O-O single bond separation of 1.49Å in H_2O_2.

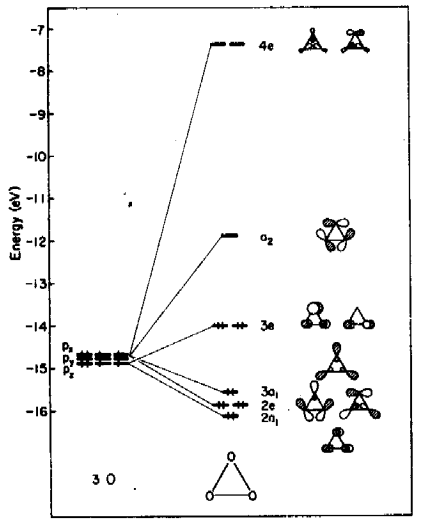

Fig.1 The energy levels of equilateral triangle ozone. The labels beside each orbital are the symmetry in C_{3V}.

The orbitals of O_3, or any cyclic X_3, have been nicely described by Gimarc[1a]. Our results, of course, follow the expectations of this work. The HOMO is a set of antibonding π^* orbitals at -14.0eV, which have e" symmetry in D_{3h} and e symmetry in C_{3v} group (3e). We will use the lower C_{3v} symmetry, since that is appropriate to the symmetry of O_3 in a complex. Below this 3e set there are 4 orbitals between -15.5eV and -16.1eV: $3a_1$ is an in-phase combination of radical p orbitals, the 2e orbitals are a mixture of tangential and radical p orbitals, $2a_1$ is the bonding π orbital. $1a_1$ and 1e orbitals are mainly linear combinations of oxygen 1s orbitals and lie below -27 eV (not shown in Fig.1). The LUMO is an out-of-phase combination of tangential p orbitals with a_2 symmetry. Above it there is an antibonding 4e set. The overlap population between two atoms is 0.3143 in O_3, a reference point we will need to use later.

The instability of cyclic O_3 is a consequence of both σ-train and lone-pair repulsion. The three highest lying oxygen lone pairs are indeed in orbitals of π symmetry. They are $2a_1$ and 3e, and 3e is O-O antibonding. Any interaction that stabilizes or depopulates the 3e π^* orbital set will stabilize O_3, increase the O-O bond order.

From the second order energy correction formula $\Delta E = \frac{|H'_{ij}|^2}{E_i - E_j}$ in perturbation

theory[4] it is clear that the ML_n fragment in hypothetical complexes of O_3 must have empty e orbitals with energy close to -14 eV and good overlap with the 3e set of O_3 fragment.

Most transition metals have d orbital energy higher than -14 eV. This is an impediment to the easy formation of a variety of cyclic O_3 complexes. Unlike ozone, for P_3 and C_3H_3 the antibonding orbitals are at -11.8 eV and -8.6 eV respectively. They have perfect match with many transition metals in energy. However, some transition metals located in the upper right corner of the transition metal part of Periodic Table, such as Ni, Co, do have d orbital energies close to -14 eV.

The overlap between O_3 HOMO and metal-ligand orbitals depends not only on the metal itself, but also on the ligands. Let us examine some cyclic O_3 complexes containing 1,2, or 3 transition metal atoms in each molecule one by one.

Mono-Metal Complexes O_3ML_n

By now the orbitals of ML_n fragments are well known, and the reader is referred to the literature for these.[5] The fragments we will discuss have one to five ligands, 6-10.

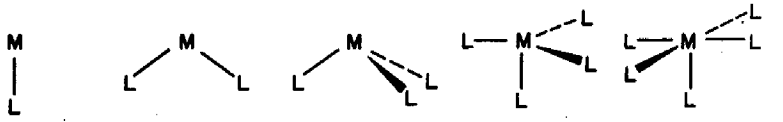

6 7 8 9 10

If we choose the symmetry axis of ML_n as the z axis, the empty e sets of ML and ML_5 are mainly metal p_x, p_y orbitals, too high in energy to interact with O_3 HOMO effectively. ML_2 does not have an empty e set. ML_3 and ML_4 do possess relatively low-lying e sets which can interact with O_3 HOMO. We discuss these two cases separately.

A single model for O_3ML_3 is a staggered $O_3NiH_3^+$, 11. Its interaction diagram is shown in Fig.2. The LUMO of NiH_3^+ is the 3e set of orbitals. Their composition is 20%(p_x or p_y of Ni)+ 12%(d_{xy} or $d_{x^2-y^2}$ of Ni)+24%(d_{yz} or d_{xz} of Ni)+44%(1s orbitals of H). Their lobes point towards the O_3 HOMO e set, with an overlap of 0.1143. The HOMO's of NiH_3^+ are a pseudo-t_{2g} set of metal d orbitals, because the three hydrogen atoms form exactly half of an octahedral ligand set. In C_{3v} symmetry they are $2a_1$ and 2e. The $2a_1$ orbital is d_{z^2}. The composition of the 2e set is 67%(d_{xy} or $d_{x^2-y^2}$)+33%(d_{yz} or d_{xz}). Its overlap with the O_3 HOMO e set is small, 0.0267, but its energy is much closer to O_3 HOMO than the 3e set of NiH_3^+. Therefore

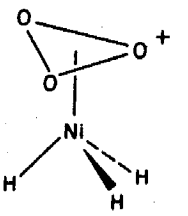

11

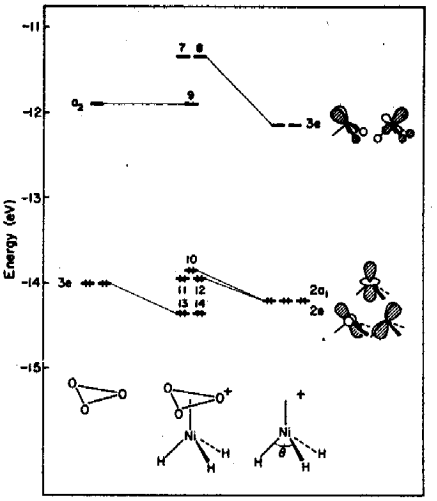

Fig.2 Interaction diagram for $O_3NiH_3^+$ with C_{3V} symmetry and H-Ni-H angles of 90°, O-Ni bond length 1.9 Å.

2e interacts substantially with the O_3 HOMO. These three e sets mix with each other forming orbitals 7 and 8, 11 and 12, 13 and 14, three e sets in the complex. The numbering here refers to Fig.2. Among them 7 and 8 are unoccupied. Orbitals 11 and 12 are combinations of O_3 HOMO (25%), NiH_3^+ 3e (15%, in-phase) and 2e (38% out-of-phase) mixing with other orbitals. Orbitals 13 and 14 are in-phase combination of the O_3 HOMO (31%), NiH_3^+ 3e (11%) and 2e (30%), mixing with other orbitals. The largest contribution of the O_3 HOMO is in orbitals 13 and 14, whose energy is 0.35 eV below O_3 HOMO. The total stabilization energy (the sum of one electron energies of the two fragments, O_3 and NiH_3^+, minus those of the $O_3NiH_3^+$ complex) is 1.75 eV. The computed overlap populations are 0.1588 between O and Ni atoms, 0.3436 between two oxygen atoms in the complex. The latter population is thus up 0.03 from 0.3143 for the isolated fragment.

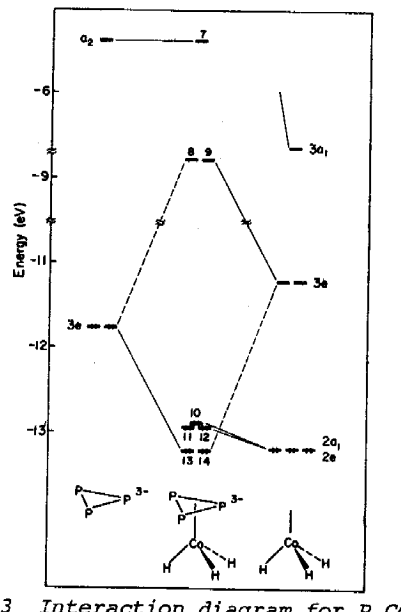

Fig.3 Interaction diagram for $P_3CoH_3^{3-}$ with C_{3V} symmetry and H-Co-H angles of 90°, P-P bond length 2.15 Å, P-Co bond length 2.3 Å.

To compare with known P_3 complexes, we did a calculation on a simple model of a P_3 complex, $P_3CoH_3^{3-}$, 12. Its interaction diagram is shown in Fig.3, and some computed indicators of binding are given in Table 1. There are many qualitative similarities between the O_3 and P_3 interaction diagrams of Figures. 2 and 3, and there are many important quantitative differences. In Fig.3 orbitals 11 and 12 are essentially the CoH_3 HOMO 2e set (71%). Orbitals 13 and 14 are in-phase combinations of P_3^{3-} HOMO's (47%), CoH_3 LUMO 3e (27%), and other orbitals. The energy difference between P_3^{3-} HOMO's and CoH_3 LUMO's is 0.6eV and their overlap is large, 0.2186. The interaction of these MO's pushes the P_3^{3-} HOMO's down by 1.46 eV and leaves

the CoH_3 HOMO 2e set very little changed in energy. The total stabilization energy upon complex formation is 5.4 eV. This large interaction energy is the reason why P_3 is so effectively stabilized by ML_3. In contrast, the energy difference between the O_3 HOMO and NiH_3^+ LUMO is 1.8 eV, and their overlap is only 0.1143. It follows that their interaction is smaller. From the complex orbital composition mentioned previously, the O_3 HOMO interacts with NiH_3 HOMO (a four electron repulsion) more than with NiH_3^+ LUMO. Therefore it is not stabilized effectively.

Perturbation theory suggests that we can improve the HOMO-LUMO interaction by lowering the ML_3 LUMO energy and/or increasing overlap. The ML_3 LUMO e set is composed in substantial part of metal d-orbitals pushed up by ligand field. If the geometry of ML_3 is changed, the energy and extent of space of those orbitals will change consequently. In the previous calculation we set $\theta=\angle LML=90°$ (see Fig.2). When this angle increases from 90°, the LUMO e set of NiH_3^+ goes down in energy. For example, their energy is lowered from -12.15 eV at 90° to -12.67 eV at 114°. One might expect a better interaction at 114° from this. But because the hydrogen ligands are closer to the xy plane where the metal atom is located, the LUMO e set has more $d_{x^2-y^2}$, d_{xy} character (33%) and less d_{xz}, d_{yz} character (9%) than in the $\theta=90°$ case, in which it has 12% of $d_{x^2-y^2}$ or d_{xy} character and 24% of d_{xz} or d_{yz} character. Meanwhile the HOMO's have more d_{xz}, d_{yz} character. So, the overlap between the O_3 HOMO with the NiH_3^+ LUMO becomes smaller, while the overlap with the NiH_3^+ HOMO becomes larger. Although orbitals 13 and 14 are at lower energy at $\theta=114°$, they mainly linear combinations of O_3 HOMO (47%) and NiH_3^+ HOMO (32%). The total stabilization energy of the complex is 1.21 eV less than in the $\theta=90°$ case (1.06 eV vs. 2.27 eV). Thus an increase of LML angle in ML_3 does not improve the stability of the hypothetical O_3ML_3 complex. On the other hand, because the ONiO angle is already much less than 90° (48.5°), it is not reasonable to decrease θ of ML_3. In a typical P_3 complex, say $(PL_3)_3Ni(P_3)Ni(PL_3)_3$, the $(PL_3)M(PL_3)$ angles are about 90°. So, in the following O_3ML_3 discussion we set θ =90°.

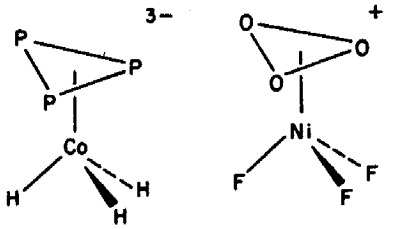

12

13

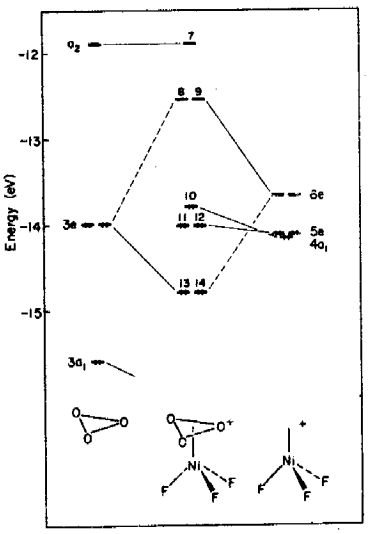

Fig.4 Interaction diagram for $O_3NiF_3^+$ with C_{3v} symmetry and F-N-F angles of 90°, O-Ni distances 1.9 Å.

The ML_3 LUMO e set is comprised of metal d-orbitals (with some p admixture) pushed up by ligand field. The energy of these orbitals will be lower if the ligand field is weak. We chose F^- ligands and did a calculation on staggered $O_3NiF_3^+$, 13. Its interaction diagram is shown in Fig.4.

The LUMO e set of NiH_3^+ was at -12.2 eV, 1.8 eV above the O_3 HOMO e set. Here the LUMO e set of NiF_3^+ is -13.7 eV, very close to -14.0 eV, the energy of the O_3 HOMO. Therefore these orbitals interact nicely and form the in-phase combinations, orbitals 13 and 14, and the unoccupied out-of-phase combinations orbitals 8 and 9. Orbitals 13 and 14 are made up of the O_3 HOMO (62%) and the NiF_3^+ LUMO (31%), and lie 0.8 eV below the O_3 HOMO. Orbitals 8 and 9 have the following composition: O_3 HOMO (36%) and NiF_3^+ LUMO (56%). Orbitals 11 and 12 are mainly the NiF_3^+ HOMO e set (88%). Orbital 10 is the metal d_{z^2} orbital pushed up 0.3eV by $2a_1$ and $3a_1$ orbitals of the O_3 fragment. The overlap populations are 0.3625 between oxygen atoms and 0.1882 between oxygen and nickel atoms. The total stabilization energy is 4.5 eV. The cyclic ozone fragment is much better stabilized in $O_3NiF_3^+$ than in $O_3NiH_3^+$.

Comparing Fig.4 and Fig.3 of $P_3CoH_3^{3-}$, we find that they have pretty much the same pattern. The O_3 or P_3 HOMO e set interacts with ML_3 LUMO and is pushed down in energy. ML_3 HOMO a_1 and e set remain almost unchanged. The O_3 or P_3 LUMO a_2 orbital remains the same. But the quantitative extent of stabilization is very much different. The P_3 HOMO is pushed down by 1.46 eV, while the O_3 HOMO is pushed down by less, 0.8 eV. The total stabilization energy is 5.4 eV for the P_3 complex and 4.5 eV for $O_3NiF_3^+$. The HOMO-LUMO gap is 4.1 eV for $P_3CoH_3^{3-}$ and 1.3 eV for $O_3NiF_3^+$. The overlap populations are different as well. In summary, substantial binding of cyclic ozone to an ML_3 moiety may be achieved, but the bonding is never as good as it is for the P_3 complex.

Still further attempts to change the ligand set included a calculation for $O_3NiCl_3^+$ and $O_3Ni(CO)_3^{4+}$. The former has a similar interaction diagram, but shows less stabilization than the F case. What interested us in the case of $O_3Ni(CO)_3^{4+}$ was that the energy of the $Ni(CO)_3^{4+}$ fragment HOMO (-14.3 eV) is lower than that of metal Ni d-orbitals. This is due to the back-bonding ability of carbonyl ligands. If carbonyl ligands are replaced by NO^+, the HOMO's are even lower. However the difference between the $M(CO)_3$ HOMO and the metal d-orbitals is still too small to make for substantial improvement in stability of the complex. Furthermore, the $Ni(CO)_3^{4+}$ LUMO e set is higher than NiF_3^+. Thus the total stabilization energy is smaller than for $O_3NiF_3^+$.

Before we leave the ML_3 complexes let us perhaps remark on the obvious. Cyclic ozone is a six-electron π-donor. This is why O_3, or the isoelectronic S_3 or P_3^{3-} will seek out a d^6 ML_3 bonding partner. The eighteen electron count at the metal is satisfied in all of these complexes.

Our next attempt to stabilize O_3 was with an ML_4 fragment. An interaction diagram for $O_3NiF_4^{2+}$ (staggered) is shown in Fig.5. The LUMO e set of the NiF_4^{2+}

fragment is mainly $d_{x^2-y^2}$ or d_{xy} (94%) on Ni. Because their overlaps with O_3 fragment orbitals are very small, these orbitals stay at almost the same energy in the complex as they were in the isolated fragment. The HOMO e set of the NiF_4^{2+} fragment is mainly d_{xz} or d_{yz} (98%). The lobes of these orbitals point towards the O_3 fragment and overlap nicely with the O_3 HOMO e set. This interaction forms two e sets in the complex. One of them is the in-phase combination of O_3 HOMO (52%) and NiF_4^{2+} HOMO's(41%) and is occupied. Its energy is 0.9 eV below the O_3 HOMO. The other is the out-of-phase combination of O_3 HOMO (45%) and NiF_4^{2+} HOMO (38%) and is empty. Here the LUMO e set of NiF_4^{2+} plays an important role. It remains constant in energy and accomodates four electrons. This makes the out-of-phase combination from HOMO-HOMO interaction empty. The total stabilization energy is 3.76 eV, and the overlap populations in the complex are 0.3642 between oxygen atoms and 0.1831 between oxygen and nickel atoms. The d^4ML_4 fragment appears to be a reasonable one for stabilizing cyclic ozone.

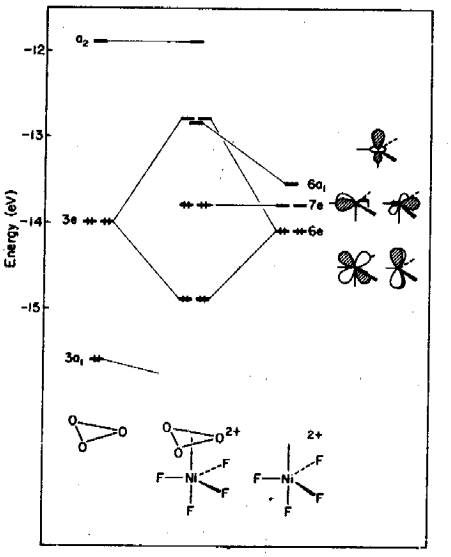

Fig.5 Interaction diagram for $O_3NiF_4^{2+}$ with C_{3v} symmetry and O-Ni distances 1.9 Å.

Di-Metal Complexes

So far we have discussed O_3 complexes with one transition metal atom. Now let us examine some complexes containing two metal atoms in each molecule. Once again the impetus for doing so comes from known P_3 complexes such as 5. Corresponding to $O_3NiF_3^+$, we did a calculation on $O_3(NiF_3)_2^{2+}$, in which the two NiF_3^+ fragments are located on the two sides of an O_3 ring, 14. If the O_3 is considered as a 6 electron donor to each metal, then both metals achieve an eighteen electron configuration.

Fig.6 is the interaction diagram for $O_3(NiF_3)_2^{2+}$. Comparing with Fig.4 we find that the two diagrams have the same pattern. The differences are that the in-phase combination of the O_3 HOMO (55%) and the two LUMO e sets of the NiF_3^+ fragment (19%×2) are 1.3 eV below the O_3 HOMO's (vs. 0.8 eV for $O_3NiF_3^+$), and that the stabilization energy is 7.8 eV (vs. 4.5 eV for $O_3NiF_3^+$). The overlap population is 0.3660 between oxygen atoms and 0.1875 between oxygen and nickel atoms.

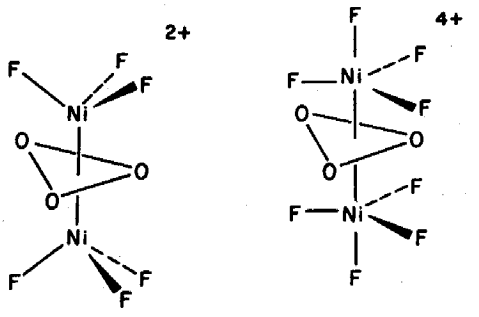

14 15

Since an ML_4 fragment was moderately successful in stabilizing O_3, we next tried $O_3(NiF_4)_2^{4+}$, 15. The results are shown in Fig.7. The orbitals numbered 18 and 19 (HOMO's of the complex) are mainly from the two HOMO e sets of $(NiF_4)^{2+}$ fragments (75%), with some mixing of $(NiF_4)^{2+}$ LUMO (19%). Orbitals 20, 21 and unoccupied orbitals 16, 17 are from the two LUMO e sets of $(NiF_4)^{2+}$. Orbitals 22 and 23 are in-phase combinations of the O_3 HOMO (48%) and the $(NiF_4)^{2+}$ HOMO (45%). Their energy is 1.3 eV below the O_3 HOMO. The total stabilization energy is 6.0 eV. The overlap populations are 0.3637 between oxygen atoms and 0.1682 between oxygen and nickel atoms.

It is clear from the above results that an O_3ML_n complex gains from interaction with a second ML_n fragment.

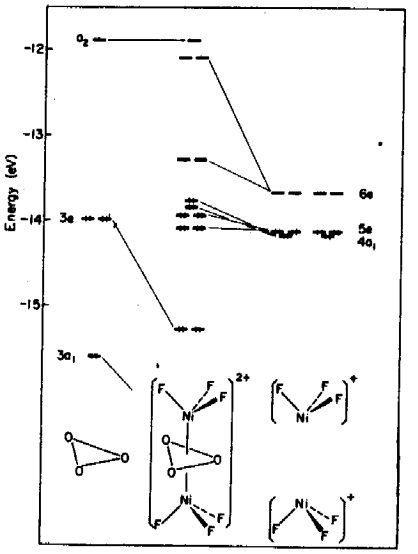

Fig.6 Interaction diagram for $O_3(NiF_3)_2^{2+}$. The energy levels on the right are those of the two separated NiF_3^+.

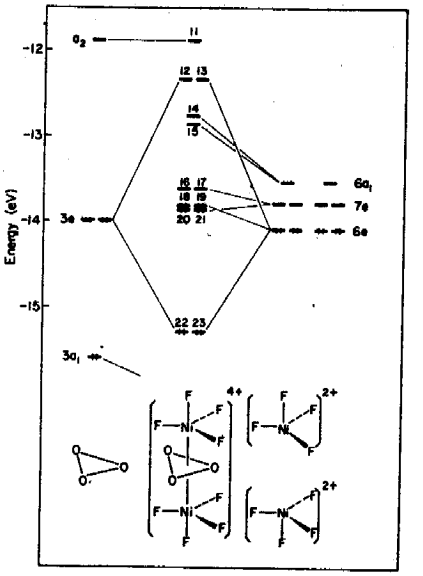

Fig.7 Interaction diagram for $O_3(NiF_4)_2^{4+}$. The energy levels on the right are those of the two separated NiF_4^{2+} fragments.

Tri-Metal Complexes

So far we focused on the HOMO e set of O_3 fragment. How about its LUMO? The a_2 orbital is an out-of-phase combination of tangential p orbitals of the oxygen atoms and 2.1 eV above its HOMO e set (see Fig.1). It has three nodal planes. But transition metal d orbitals do not contain any orbital of such symmetry and, therefore, do not interact with the a_2 at all. Some of the f orbitals of the lanthanide and actinide elements are of a_2 symmetry. We tried some calculations with such elements, but found little a_2 interaction, even when allowed by symmetry.

When some ligands are attached to the metal, as in NiF_3^+ or $Ni(CO)_3^{4+}$, there arises an a_2 combination from ligand p orbitals. But its overlap with O_3 a_2 is

small, and they are far removed in energy.

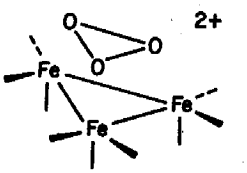

16

The problem of finding an interaction partner with an orbital of a_2 symmetry can be approached, however, by introducing a metal cluster with C_{3v} symmetry, such as $Fe_3(CO)_9$.[7] An interaction diagram for $O_3Fe_3(CO)_9^{2+}$, 16 is shown in Fig.8. The orbitals of the $Fe_3(CO)_9^{2+}$ fragment shown in Fig.8, are mainly metal d orbitals. Among them there are two a_2 orbitals. The upper one is an out-of-phase combination of d_{xy}, $d_{x^2-y^2}$ orbitals and is too high in energy to interact with the O_3 a_2 orbital. The lower one shown in Fig.9, consist of three tangential d orbitals which are linear combinations of d_{xz} and d_{yz} orbitals. This a_2 orbital interacts with the O_3 LUMO and forms an in-phase combination consisting of 13% O_3 LUMO and 87% of the Fe_3 fragment a_2 orbital. As a result of this interaction this orbital is pushed down by 0.2 eV. For the complex $O_3Fe_3(CO)_9^{2+}$ the total stabilization energy is 3.18 eV. In this complex the total electron number is 46, 2 electrons less than 18 electrons per Fe atom.

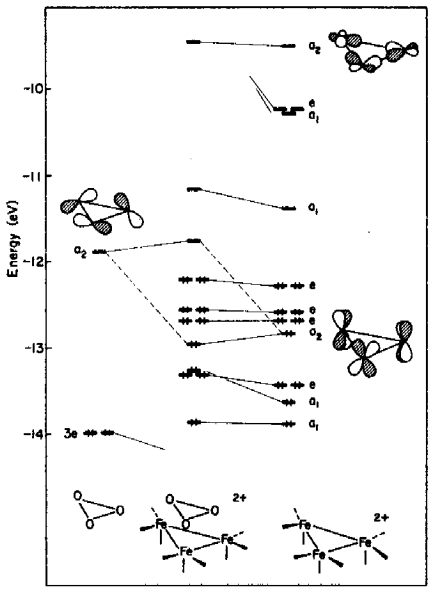

Fig.8 Interaction diagram for $O_3Fe_3(CO)_9^{2+}$ with C_{3v} symmetry. The geometric parameters are specified in Appendix.

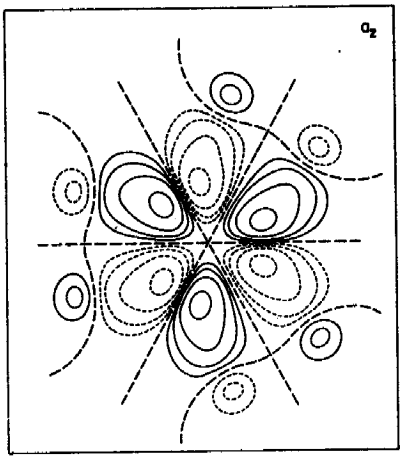

Fig.9 Contour plot of the low-lying a_2 orbital in the plane which is parallel to the three metal plane and 1 Å above it. The contours have the values 0.04, 0.02, 0.01, 0.005 and 0.0. The dotted and full lines refer to opposite signs of Ψ and the dashed lines are nodal contours.

From this example we see that a metal cluster with a certain geometry matches the symmetry requirements of the O_3 fragment. Perhaps some metal surface can play a similar function.

Concluding Remarks

WE have examined the possibility of the existance of a cyclic ozone structure in

transition metal complexes. The study is in no way complete, or definitive, for extended Hückel calculations are not suitable for geometry optimization. Nor have we probed at all the most common fate of transition metal systems with high oxygen content, namely O-O bond cleavage to give oxo complexes with metal-oxygen bonds of multiplicity greater than one.

What we can say, however, is that in principle, the cyclic O_3 unit is capable of being stabilized by certain specific $d^6 ML_3$ and ML_4 units, as well as by some dinuclear and trinuclear metal units. Its stabilization is less than that of the similar P_3^{3-} unit, for reasons of energy mismatch and poor overlap with most ML_n units. Nevertheless we believe that with an appropriate ligand one will someday find a bound cyclic ozone or SO_2, or S_3.

Acknowledgment

WE are grateful to the members of our group for numerous discussions and to Jane Jorgensen for the drawings and Eleanor Stolz for the typing. Our research was supported by the National Science Foundation through Research Grant CHE 7828048.

Appendix

THE orbital exponents and H_{ii}'s for the extended Hückel calculations[8] were obtained from earlier work[9] and are listed in Table 2. The assumed bond length between the oxygen atoms in O_3 is 1.5 Å, the P-P bond length in P_3 was taken as 2.15 Å. Metal-ligand bond lengths in ML_n are 1.542 Å(M-H), 1.99 Å(Ni-F), 2.32 Å(Ni-Cl) and 1.80 Å(Ni-CO). The O-Ni bond length is 1.9 Å and P-Co bond length is 2.3 Å. The basic geometry of $Fe_3(CO)_9$ consisted of an equilateral triangle of Fe atoms with an Fe-Fe distance of 2.64 Å. Fe-C bond length is 1.86 Å and the Fe-O distance is 2.1 Å. In $O_3Fe_3(CO)_9^{2+}$ O_3 and Fe_3L_9 are eclipsed and the two equatorial carbonyls bonded to the same Fe atom separated by an angle of 115°.

Table 1. Calculated Stabilization Energies and Overlap Populations

Complex	Total Stabilization Energy eV	Overlap Population Between O - O	O - M
Free Cyclic O_3	---	0.3143	------
$O_3NiH_3^+$ ($\angle$HNiH=90°)	2.3	0.3436	0.1588
($\angle$HNiH=114°)	1.1	0.3501	0.1536
$P_3CoH_3^{3-}$	5.4	0.7060*	0.2571*
$O_3NiF_3^+$	4.5	0.3625	0.1882
$O_3NiF_4^{2+}$	3.8	0.3642	0.1831
$O_3(NiF_3)_2^{2+}$	7.8	0.3660	0.1875
$O_3(NiCl_3)_2^{2+}$	6.2	0.3638	0.1798
$O_3(NiF_4)_2^{4+}$	6.0	0.3637	0.1682
$O_3Fe_3(CO)_9^{2+}$	3.2	0.3087	0.2898

* *These are overlap populations between P atoms in $P_3CoH_3^{3-}$ and between P and Co atoms. The reference overlap population between two P atoms in free P_3^{3-} is 0.5653.*

Table 2. Parameters Used in Extended Hückel Calculations

Orbital		H_{ii} eV	ζ_1	ζ_2	C_1[a]	C_2[a]
H	1s	-13.6	1.3			
C	2s	-21.4	1.625			
	2p	-11.4	1.625			
N	2s	-26.0	1.95			
	2p	-13.4	1.95			
O	2s	-32.3	2.275			
	2p	-14.8	2.275			
F	2s	-40.0	2.452			
	2p	-18.1	2.452			
P	3s	-18.6	1.60			
	3p	-14.0	1.60			
Cl	3s	-30.0	2.033			
	3p	-15.0	2.033			
Fe	3d	-12.70	5.35	1.80	0.5366	0.6678
	4s	-9.17	1.90			
	4p	-5.37	1.90			
Co	3d	-13.18	5.55	2.10	0.5679	0.6059
	4s	-9.21	2.00			
	4p	-5.29	2.00			
Ni	3d	-14.2	5.75	2.30	0.5798	0.5782
	4s	-10.95	2.1			
	4p	-6.27	2.1			

[a] *These are the coefficients in the double ζ expansion.*

REFERENCES

1. (a) Gimarc,B.M. "Molecular Structure and Bonding", Academic Press, New York, (1979).
   (b) Peyerimhoff,S.D. and Buenker,R.J., J. Chem. Phys., 47, 1953 (1967).
   (c) Hay,P.J., Dunning,T.H. and Goddard,W.A., Chem. Phys. Lett., 23, 457 (1973).
   (d) Shih,S., Buenker,R.J. and Peyerimhoff,S.D., Chem. Phys. Lett., 28, 463 (1974).
   (e) Hayes,E.F. and Pfeiffer,G.V., J. Am. Chem. Soc., 90 4773 (1968).
   (f) Harding,L.B. and Goddard,W.A., III, J. Chem. Phys., 67, 2377 (1977).
2. (a) Sharpless, K.B., Townsend, J.M. and Williams, D.R., J. Am. Chem. Soc., 94, 295(1972).
   (b) Postel, M., Brevard, C., Arzoumanian, H. and Riess, J.G., J. Am. Chem. Soc., 105, 4922(1983).
3. (a) Vaira,M.Di, Ghilardi,G.A., Midollini,S., Sacconi,L., J. Am. Chem. Soc., 100, 2550 (1978).
   (b) Vaira,M. Di, Midollini,S. and Sacconi,L., J. Am. Chem. Soc., 101, 1757 (1979).
   (c) Bianchini,C., Viara,M. Di, Meli,A. and Sacconi,L., J. Am. Chem. Soc. 103, 1448 (1981).
   (d) Dapporto,P., Sacconi,L., Stoppioni,P. and Zanobini,F., Inorg. Chem., 20, 3834 (1981).
   (e) Di Vaira, M., Sacconi, L. and stoppioni, P., J. Org. Chem., 250, 183(1983).
4. (a) Salem,L., J. Am. Chem. Soc. 90, 543 (1968).
   (b) Fukui,K. and Fujimoto,H., Bull. Chem. Soc., Jap., 41, 1989 (1968).
5. (a) Elian,M. and Hoffmann,R., Inorg. Chem., 14, 1058 (1975).
   (b) Burdett,J.K., "Molecular Shapes", Wiley, New Yoek (1980).
   (c) Albright,T.A., Tetrahedron,38, 1339 (1982).
6. Viara,M. Di, Ghilardi,C.A., Midollini,S., Sacconi,L., J. Am. Chem. Soc., 100, 2550 (1978).
7. Schilling, B., E.R. and Hoffmann, R., J. Am. Chem. Soc., 101, 3456 (1979).
8. (a) Hoffmann,R., J. Chem. Phys. 39, 1397 (1963).
   (b) Hoffmann,R. and Lipscomb,W.N., ibid. 36, 2179, 3489 (1962) 37, 2872 (1962).
9. (a) Summerville,R.H. and Hoffmann,R., J. Am. Chem. Soc. 98, 7240 (1976).
   (b) Albright,T.A., Hofmann,P. and Hoffmann,R., ibid. 99, 7546 (1977).